Journal Pre-proof

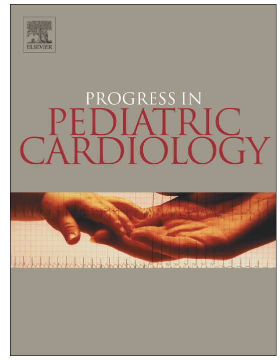

Echocardiographic assessment of ventricular function: Conventional and advanced technologies and their clinical applications

Takeshi Tsuda, Daphney Kernizan, Erica Del Grippo, Deepika Thacker, Rami Kharouf, Shubhika Srivastava

PII: S1058-9813(20)30138-7

DOI: https://doi.org/10.1016/j.ppedcard.2020.101269

Reference: PPC 101269

To appear in: *Progress in Pediatric Cardiology*

Received date: 4 June 2020

Revised date: 25 June 2020

Accepted date: 29 June 2020

Please cite this article as: T. Tsuda, D. Kernizan, E. Del Grippo, et al., Echocardiographic assessment of ventricular function: Conventional and advanced technologies and their clinical applications, *Progress in Pediatric Cardiology* (2020), https://doi.org/10.1016/j.ppedcard.2020.101269

Progress in Pediatric Cardiology

Echocardiographic Assessment of Ventricular Function:

Conventional and Advanced Technologies and their Clinical Applications

Takeshi Tsuda[1,2]†, Daphney Kernizan [1,2], Erica Del Grippo[1,2], Deepika Thacker[1,2],

Rami Kharouf[1,2], Shubhika Srivastava[1,2]

[1]Nemours Cardiac Center, Nemours/Alfred I duPont Hospital for Children

Wilmington, DE 19803

[2] Department of Pediatrics, Sidney Kimmel Medical College at Thomas Jefferson University

Philadelphia, PA 19107

†Corresponding Author:

Takeshi Tsuda, MD, FAAP, FACC

Nemours Cardiac Center, Nemours/Alfred I. duPont Hospital for Children

1600 Rockland Rd, Wilmington, DE 19103

TEL: (302)651-6677 FAX: (302)651-6601 Email: ttsuda@nemours.org

Abstract

Echocardiogram is the first-line and most used noninvasive imaging diagnostic modality and is convenient and reliable in its assessment of ventricular function in pediatrics. Ventricular function is an important physiological parameter representing myocardial performance in response to overall hemodynamic status. Here, we introduce basic principles of conventional echocardiography and advanced echocardiographic technology, including tissue Doppler imaging, 3-dimensional echocardiogram, and speckled tracking echocardiography. Then, we overview clinical applications of these methods in assessing ventricular function in pediatrics, including single ventricle after staged surgical palliation, right ventricular dysfunction in pulmonary hypertension, and ventricular-ventricular interactions in various heart disease. With multimodality approaches, the advantages and limitations of echocardiographic assessment of ventricular function are discussed.

Keywords

Single ventricle, pulmonary hypertension, speckle tracking echocardiography, strain, ventricular-ventricular interaction

1. Introduction

Echocardiographic assessment of ventricular function is an integral part of daily cardiology practice as it reliably provides qualitative and quantitative measure of myocardial performance (systolic and diastolic function) and overall hemodynamic status (stroke volume, preload, and afterload), and serves as a predictor of clinical outcomes (disease progression, recovery, and prognosis). Because of its convenience and reliability, echocardiogram remains the most widely used diagnostic modality in pediatric cardiology. In addition, recent advances in assessment of tissue motion and deformation have provided several exciting new capacities in interpreting ventricular function noninvasively. However, they do have certain important limitations. Ventricular global performance is influenced by myocardial contractility, preload, afterload, and heart rate. A load independent assessment of myocardial performance or contractility is difficult to assess by any one parameter. Often, reporting of global ventricular performance has to consider the underlying loading conditions.

In this review paper, we first overview basic principles of conventional echocardiography and newly introduced advanced echocardiographic technologies. Then, we discuss how these modalities are utilized in assessing ventricular function in certain unique problems commonly encountered in pediatric cardiology, including single ventricle, pulmonary hypertension, and ventricular-ventricular interactions.

2. Conventional Approach in Assessing Ventricular Function

Conventional echocardiographic approaches include 2-dimensional echocardiography, M-mode, pulsed Doppler, and color Doppler studies. Lopez et al. described standards of quantification of ventricular function [1], and a recent publication by Frommelt et al. questioned the reliability in standard 2-DE methods of quantitation of ventricular function [2].

2-1 Left Ventricle

2-1-1 *Systolic Function*

Shortening fraction and ejection fraction are geometric parameters that characterize dimensional or volumetric changes during the cardiac cycle [3]. Shortening fraction is the percentage change in left ventricular (LV) dimension in M-mode at the level of the papillary muscles using the parasternal short-axis views.

$$\%SF = (LVEDD - LVESD)/LVEDD \times 100$$

SF: shortening fraction, LVEDD: LV end-diastolic dimension, LVESD: LV end-systolic dimension

Normal LV function varies with age, and multiple Z-score methods have been described to define normative values of SF ranging from a normal value of $\geq$ 35% in neonates to $\geq$ 28% in adolescents [4, 5] M-mode cannot be used when ventricular septal geometry is not convex as in right ventricular (RV) volume or pressure load or septal dyskinesis.

Ejection fraction is the percentage change in LV volume from end-diastole to end-systole.

$$\%EF = (LVEDV - LVESV)/LVEDV \times 100$$

EF: ejection fraction, LVEDV: LV end-diastolic volume, LVESV: LV end-systolic volume

The methods most commonly used are the modified Simpson's method or disk summation method [1, 4] and 5/6 area x length method [6]. In the Simpson's method, the LV endocardial border is traced in two orthogonal planes from the apical 4-chamber and apical 2-chamber views. A computer algorithm then divides the traced area into 20 discs of equal height and sums the volume of each disc [7]. Like shortening fraction, ejection fraction is dependent on preload, afterload, and LV geometry. Ejection fraction, however, additionally takes regional dysfunction into account in assessing global function, whereas shortening fraction measurements become unreliable when regional septal hypokinesia or dyskinesia is present [8]. Normal LV function is suggested by ejection fraction greater than 55% in older children and adults [4, 5]. The 5/6 area x length method uses the length from apical views and the cross-sectional area from the parasternal short axis view at the level of the papillary muscle. Lee et al. demonstrated reliability of the 5/6 area x length method in assessment of ventricular size and function in dilated ventricles with aortic regurgitation [9]. This method has demonstrated reliability in assessment when LV geometry is altered, as in tetralogy of Fallot [10].

Systolic-to-diastolic time duration ratio has been described by Friedberg in multiple applications for LV, RV, and single ventricles [11]. As global performance deteriorates, it is at the expense of shortening of diastole that leads to increase in systolic to diastolic time duration ratio. This ratio can be derived from pulsed Doppler interrogation of atrio-ventricular valve regurgitation or from tissue Doppler imaging (TDI).

In presence of mitral regurgitation, the rate of pressure rise in early systole (dP/dT max) in continuous wave Doppler may be used to evaluate global LV contractility. Mitral regurgitation jet velocity depends on the pressure gradient between the LV and left atrium (LA). As there is no significant change in LA pressure during isovolumetric contraction, mitral regurgitation dP/dT reflects LV pressure changes, a time duration between change of velocity from 1 to 3 m/s on the mitral regurgitation spectral. The normal value of mitral regurgitation dP/dT is $\geq$ 1,000–1,200 mmHg/s, and a value of <500 mmHg/s is indicative of severe systolic dysfunction [12].

2-1-2 *Myocardial Performance Index*

Myocardial performance index (or Tei index) is a global measure of ventricular function which combines both systolic and diastolic function. The MPI incorporates the intervals of both isovolumetric contraction time and isovolumetric relaxation time, which correspond to periods of active chamber contraction and early relaxation, respectively. The myocardial performance index can be calculated using Doppler echocardiography measuring time intervals from mitral and aortic traces [13].

$$MPI = (ICT + IRT)/ET$$

MPI: myocardial performance index, ICT: isovolumetric contraction time,

IRT: isovolumetric relaxation time, ET: ejection time

There are variable changes with progressive myocardial systolic dysfunction where the sum of isovolumetric contraction time and isovolumetric relaxation time progressively lengthens as ventricular dysfunction evolves and ejection time is shortened. Diastolic dysfunction results in prolongation of isovolumetric contraction time. Thus, with worsening LV dysfunction, (isovolumic contraction time + isovolumetric contraction time)/ejection time increases disproportionately to any change in the individual components of the index. Normal values for the LV and RV are 0.35 ± 0.03 and 0.28 ± 0.04, respectively [8]. The myocardial performance index is independent of ventricular geometry but dependent on preload and afterload; it does not specify systolic or diastolic dysfunction [8].

2-1-3 *Diastolic function*

Many factors influence ventricular diastolic filling, including ventricular systolic function, atrioventricular valve function, rate of ventricular relaxation, the passive compliance or stiffness of the atrial and ventricular muscle, atrial systolic function, the loading or volume conditions of the two chambers, intrathoracic pressure changes with respiration, and the heart rate and rhythm [14, 15]. Diastolic function can be categorized as impaired relaxation and impaired compliance with or without elevated left atrial (LA) pressure. Trans-mitral Doppler inflow patterns assess early filling (E wave) and late filling (A wave) velocities [16]. They are measured in an apical four-chamber view and are used to derive the ratio of these two velocities (E/A). Pulsed-wave Doppler patterns of pulmonary venous inflow complements mitral valve inflow patterns and includes peak systolic (S wave) and diastolic (D wave) velocities [17, 18]. The velocity and duration of atrial reversal (A wave) are seen in late diastole with atrial contraction and may reflect elevated LV end-diastolic filling pressure [14, 19]. The pattern of ventricular filling can also be visualized by M-mode assessment of early diastolic flow propagation velocity from the atrioventricular valve to the apex using flow color Doppler [20]. As relaxation becomes abnormal, the rate of early diastolic flow propagation into the ventricle slows, and this decrease can be measured as the slope. The higher the slope, the faster the flow propagation and the more rapid the ventricular relaxation [20, 21]. Previous studies have questioned if adult models of diastolic dysfunction are applicable to children, and published normal data for children often present a wide range of normal values [22-25].

The authors believe that septal E' and lateral annular E' velocities, increased deceleration time, and IVRT can be used to assess impaired relaxation and presence of mid diastolic L' wave, increased velocity of atrio-systolic flow reversal on the pulmonary vein Doppler, and increased LA size as markers for increased LA and LV end diastolic pressure or poor LV compliance. Sasaki et al. have shown that children can have poor LV compliance and elevated LA pressures with restrictive cardiomyopathy, even with normal E' [26]. The authors use LA dilation and at least two other abnormalities to diagnose diastolic dysfunction with elevated LA pressure or poor compliance. Ratios of E/E' and other individual indices can be used to trend diastolic function over time using the patient as their own control.

2-2 Right ventricle

Right ventricle is composed of an inflow tract, trabeculated apex, and outflow tract; it has a trigonal pyramidal shape, whereas LV has a symmetric cone shape. Right ventricular contraction occurs from the inflow tract to the apical trabecular zone; it then reaches the outflow tract [27] and is predominantly longitudinal [28, 29]. However, the approach of RV free wall toward the septum, septal contraction, regional RV free-wall deformation, RV free-wall regional function, and septal-to-RV free wall synchrony all contribute to RV performance [30]. Conventional assessment of RV function is obtained through myocardial performance index, fractional area change, and tricuspid annular systolic excursion. Other parameters include RV wall thickness, RV systolic pressure estimate, dP/dT of RV, right atrial (RA) size, and RV diastolic filling [28]. Detailed discussion of RV function is also discussed in 4-2 "Pulmonary Hypertension and RV Dysfunction".

2-2-1 *Myocardial Performance Index*

The myocardial performance index can be measured with tricuspid valve inflow, which indicates both systolic and diastolic function of the ventricles independent of ventricular geometry or loading status [31, 32]. Abnormally elevated RV myocardial performance index was noted after Senning operation for d-transposition of the great arteries [31] and unrepaired congenital corrected TGA [32] when compared with control children. The normal value range is from 0.15 to 0.40 in healthy adults, and > 0.5 suggests RV functional impairment [1].

2-2-2 *Fractional Area Change*

The fractional area change gives an estimate of global RV systolic function. Right ventricular long axis area is measured by tracing the endocardial border by planimetry and is defined as:

$$\%FAC = (RVEDA – RVESA)/RVEDA \times 100\%$$

FAC: fractional area change, RVEDA: RV end diastolic area, RVESA: RV end systolic area

An RV fractional area change < 35% indicates RV systolic dysfunction [4]. However, unlikely LV, fractional area change has a limited value because of the complex geometry of RV.

2-2-3 Tricuspid annular plane systolic excursion

The tricuspid annular plane systolic excursion is calculated by measuring the excursion of the tricuspid valve annulus by M-mode rendering at the free-wall side in the four-chamber view [33]. It is a measure of longitudinal RV function, as longitudinal shortening is an important fiber orientation in the RV wall [8] and has shown good correlations with parameters estimating RV global systolic function [4]. A tricuspid annular plane systolic excursion calculation of < 17mm is highly suggestive of RV systolic dysfunction in adults [4]. In 405 asymptomatic Spanish children ranging from newborn to 18 years of age, the reference value of tricuspid annular plane systolic excursion was reported from 10.56 ± 3.96 mm in newborns to 20.95 ± 6.54 mm in the 13 to 18 year-old group [34].

3. Advanced Echocardiographic Technology

3.1 *Three-dimensional echocardiography*

Three-dimensional assessment of ventricular volumes and function is a reliable and reproducible technology that is increasingly being used to plan and guide patient management [35-38]. Suitable spatial and temporal resolution in 3-dimensional echocardiography is a priority for imaging of congenital heart disease, particularly valve pathology and complex lesions [39]. The matrix transducer has different modalities of data acquisition whose use is dictated by the clinical question [40]. The ability to assess cardiac function depends on the detection of the endocardial and/or epicardial border. Three-dimensional echocardiography tracking algorithms for calculating volumes represent a wide spectrum ranging from fully automated to manually based algorithms [41].

The capability of 3-dimensional echocardiography to capture the entire LV volume offers the opportunity to assess global and regional LV function. Ventricular dyssynchrony is expressed as the time taken to reach minimum regional volume for each segment as a percentage of the cardiac cycle. It is the standard deviation of the time taken for segments to reach their minimum systolic volume, indexed to the cardiac cycle length, known as the systolic dyssynchrony index [42]. Higher systolic dyssynchrony index denotes increasing intraventricular dyssynchrony [42]. Current software packages define abnormal wall motion with respect to the central LV axis, which has limitations for some congenital heart disease patients with an LV of unusual shape [39].

3.2 *Tissue Doppler Imaging*

Tissue Doppler imaging involves pulsed wave Doppler interrogation of myocardial motion rather than blood flow [1]. Primary measurements include the systolic, early diastolic, and late diastolic velocities [43]. The sample volume is placed within the myocardial tissue immediately adjacent to the septal and lateral hinge points of the mitral valve, and velocities are measured [7]. Once mitral inflow, annular velocities, and time intervals are acquired, it is possible to compute additional time intervals and ratios that quantify ventricular diastolic function and prediction of LV filling pressures [18]. In addition to its dependency on age, heart rate, geometry and loading conditions, its main drawbacks are the limitations of pulsed wave Doppler including angle dependency and the inability to differentiate the velocity generated by actual myocardial contraction and the velocity produced by translational motion by akinetic myocardial segments when they get pulled by the adjacent normally contracting myocardium [5, 8].

3.3 *Strain and Strain Rate*

Traditional methods of ventricular function assessment are based on endocardial excursion and thickening of myocardium [4]. These methods do not account for passive motion and tethering of segments. Strain and strain rate are mechanical engineering principles, initially studied in isolated heart muscle and intact animal hearts, introduced the principles of stress, stain, and stiffness [44]. Noninvasive strain imaging in humans was first performed using magnetic resonance imaging with magnetic resonance tagging sequences [45, 46]. Strain (ε) is defined as the change of length of an object or deformation of the object normalized to its original length: $\varepsilon = (L-L_0)/L_0$, where L is the final length and L_0 is the initial length of the object being measured; strain rate is the rate of change of strain and is measured in $second^{-1}$

[47]. Strain and strain rate obtained from apical views are represented by negative values (%) as myocardium shortens in this longitudinal dimension. Other views that can be used to obtain strain are the parasternal short axis at the papillary muscle level, where two strain values can be obtained: circumferential strain (shortening during systole with a negative value) and radial strain (myocardial wall-thickening with a positive value) [48].

There are two main methods of measuring strain and strain rate: tissue Doppler imaging and speckle tracking echocardiography. The tissue Doppler imaging method requires high frame rates (usually above 100 frames per second) and, because it is Doppler based, is angle-dependent and can obtain the strain rate in only one direction that is parallel to ultrasound beam [49]. The other disadvantage is that this method cannot distinguish between active myocardial motion and passive motion that results from tethering of diseased myocardium to surrounding normally functioning myocardium [50]**.** On the other hand, speckle tracking echocardiography is not angle-dependent and allows calculation of strain and strain rate in longitudinal, circumferential, and radial directions. It also requires high frame rates but less than what is required in tissue Doppler imaging. Normal values for tissue-Doppler [51, 52] and speckle tracking echocardiography-derived strain [53-55] have been established for adults and children. The superiority of strain and strain rate imaging to conventional echocardiographic measures of ventricular function has been shown in multiple studies. In children following orthotopic heart transplantation, speckle tracking echocardiography-derived LV strain was abnormal in acute rejection even in the absence of other changes in functional parammeters like shortening fraction, tissue Doppler imaging, or myocardial performance index [56]. In pediatric patients with acute leukemia, strain values were acutely reduced shortly after administration of anthracyclines, which correlated with the cumulative anthracycline dose used [57]. Despite normal ejection fraction or shortening fraction, global longitudinal and circumferential strains were abnormal in patients with Duchenne muscular dystrophy compared with controls, suggesting that strain can detect early myocardial dysfunction [58]. In addition, speckle tracking echocardiography-derived strain has been studied in pediatric patients following cardiac surgery;

significant changes in longitudinal and circumferential strain in the immediate post-operative period correlated well with duration of aortic cross-clamp time despite no significant change in shortening fraction or ejection fraction [59].

3.4 Left Ventricular Torsion and Rotation

Echocardiographic assessment of LV torsion is a novel methodology for assessment of LV function. In systole, the LV apex rotates counterclockwise when viewed from the apex, while the base rotates clockwise. This creates a torsional deformation from the dynamic interaction of the oppositely wound epicardial and endocardial myocardial fiber helices. This systolic twisting and early diastolic untwisting creates a wringing motion, which is then measured using LV torsion imaging with speckle tracking or tissue Doppler imaging [60, 61].

The LV rotation and LV rotation velocity are defined as angular displacement and velocity, respectively, of the LV about its central axis in the short-axis image. They are measured in degrees (^{o}) and degrees/sec ($^{o/s}$), respectively. Counterclockwise LV rotation as viewed from the apex is expressed as a positive value. The LV torsion and LV torsion velocity are then reported as the net difference between apical and basal short-axis planes [61]. Absolute values of LV torsion increase with age. Left ventricular torsion imaging, while not a part of routine assessment of ventricular function in children, has been used in several different pathological conditions, including dilated cardiomyopathy [62], aortic stenosis [63], and anthracycline cardiotoxicity [64].

Clinical applications of these modalities, conventional and advanced, are summarized in Table 1 (systolic function) and Table 2 (diastolic function).

4 Assessing Ventricular Function in Special Conditions in Pediatrics

4-1 Single Ventricle after Fontan Operation

4-1-1 *Surgical Palliation of Single Ventricle*

Pediatric patients with single ventricular anatomy commonly undergo staged surgical palliation with completion of Fontan operation [65]. Upon Fontan completion, the entire pulmonary blood flow is supplied directly by systemic venous return while a single ventricle generates systemic cardiac output with nearly normal arterial oxygenation saturation. As the result, central venous pressure increases with non-pulsatile pulmonary blood flow. Fontan circulation is not only a single ventricular circulation but one of inherently and simultaneously decreased ventricular preload and increased afterload [66]. Peak exercise capacity is generally decreased (approximately 60% of normal) in Fontan patients [67].

4-1-2 *Hemodynamic Abnormalities after Fontan Completion*

Although the development of the staged surgical palliation has improved life expectancy, patients with single ventricle are still at risk for progressive heart failure and death [68], especially those with single RV as RV is morphologically not capable of dealing with chronic exposure to the high afterload of the systemic circulation [69]. Although ventricular systolic function was overall preserved in most of pediatric patients after Fontan operation [70], many of these patients with functional single RV due to hypoplastic left heart syndrome develop ventricular mechanical dyssynchrony, likely contributing to their RV dysfunction [71]. Rosner et al. reported that a classic-pattern of dyssynchrony was noted in 15% of 100 Fontan patients; it was commonly associated with more dilated ventricles with reduced systolic and diastolic function [72]. Increased aortic stiffness and afterload due to aortic arch reconstruction also affects ventricular performance [73].

4-1-3 *Echocardiographic Assessment of Single Ventricular Function*

Commonly used methods include annular plane displacement, systolic-to-diastolic time duration ratio, peak systolic annular velocity (S’), and longitudinal and circumferential strain measurements in single RV and traditional methods of LV function assessment in single LV.

a) Systolic function

Echocardiography, when used correctly, can be a great tool for systolic and diastolic function assessment. However, the unique anatomy of single ventricles can sometimes pose challenges with echocardiographic assessments by standard measurements and protocols of ventricular function. Echocardiography can provide essential information together with other imaging modalities for accurate assessment [74].

Ventricular systolic function of single ventricle is an important parameter to address myocardial healthiness that is influenced by baseline myocardial mechanics, ventricular geometry, secondary myocardial fibrosis, and loading condition. Ventricular function has been shown to be decreased when compared with normal control patients in both single RV and single LV [75]. Single LV showed diminished ejection fraction by biplane Simpson's method and reduced basal circumferential deformation and basal rotation with preserved global longitudinal deformation when compared with control LV [76]. Significant differences in strain analysis were noted between single LV and normal biventricular LV due to spherical ventricular geometry [77]. Three-dimensional speckle tracking echocardiography of single LV demonstrated increased mechanical dyssynchrony and myocardial deformation that correlated well with LV ejection fraction and myocardial performance index [78, 79].

A standardized protocol to assess quantitative RV function by 2-dimensional echocardiography with ideal inter-observer reliability is lacking because of its unique geometry [40]. Compared with normal control RV, single RV after Fontan revealed decreased strain, strain rate, and longitudinal displacement and increased dyssynchrony [80]. Higher incidence of both systolic and diastolic dysfunction was found in single RV when compared with single LV [81], which is associated with worse clinical outcome in single RV after Fontan completion [82]. In 41 patients with HLHS after Fontan operation, systolic function represented by fractional area change showed an excellent correlation with myocardial performance index, RV global longitudinal strain, and tissue annular displacement of the tricuspid valve [83]. When comparing normal controls with single RV physiology, Hershenson et al. demonstrated RV free wall peak systolic annular velocity (s) to be lower [75]. In patients with hypoplastic left heart syndrome, global longitudinal strain rate derived by STE correlated with intrinsic measures of myocardial contractility during cardiac catheterization-obtained conductance catheter techniques [84].

Systolic function by measurement of torsion has be noted to be similar when compared with controls. In a study by Grattan, the overall torsion of those patients with single ventricles was comparable to their control patients [85] This study demonstrated a decrease or reverse in basal torsion with a compensatory apical torsion. Utilizing 3-dimensional echocardiography has also been studied in the single-ventricle population. In single RV anatomy, the use of 2-dimensional echocardiography to qualify function of the RV is difficult and not always reliable. Sato et al. demonstrated the usefulness of 3-dimensional speckle tracking echocardiography in hypoplastic left heart syndrome after the Fontan, showing a positive relationship between global principal strain and 3-dimensional ejection fraction [86].

b) Diastolic function

Diastolic function is altered in patients with single ventricles after the Fontan procedure, although the mechanisms of diastolic dysfunction are not entirely clear [70]. Serial Doppler diastolic filling assessment of the patients with single ventricle showed an inherent but diastolic dysfunction after Fontan completion [87]. There are few studies showing true correlation between diastolic function on echocardiographic assessment and measured ventricular filling pressure by cardiac catheterization in patients with single ventricle. Functional single ventricular anatomy is at risk for elevated end diastolic pressure in both the second- and third-stage palliation surgeries. This increase in end diastolic pressure mitigates passive flow through the pulmonary arteries, which is needed for this type of circulation. Cardiac catheterization remains the standard for presurgical assessment of this, although echocardiogram can also be used. When comparing cardiac catheterization findings with echocardiography, a study by Menon et al. found tissue Doppler imaging and pulmonary vein Doppler to be correlative to cardiac catheterization [88]. Their study examined patients prior to the second and third stages of surgical palliation and found the end diastolic pressure obtained on the cardiac catheterization had a positive correlation with E’, pulmonary atrial reversal duration, and E/E’ ratio obtained by pulsed Doppler. In contrast, a recent study by Goudar et al. reported no statistically significant correlation between the echocardiographic parameters including pulmonary vein a-wave duration, tissue Doppler velocities (E, E’, and S’), and E/E’, and end diastolic pressure obtained at cardiac catheterization [89]. Margossian et al. demonstrated a high incidence of diastolic dysfunction in patients with single ventricle by echocardiogram but without significant correlation with clinical outcomes (i.e., exercise capacity), suggesting that the methodology developed for echocardiographic assessment of diastolic function in adults with biventricular hearts may not be applicable to pediatric single-ventricle patients [90].

c) Other factors affecting ventricular function in Fontan circulation

Surgical palliation for hypoplastic left heart syndrome commonly requires complex arch reconstruction at the first palliation (Norwood), which increases arterial elastance or afterload, resulting in ventricular dysfunction in single RV after Fontan operation compared with single LV [91]. Even without arch reconstruction, Fontan circulation is associated with increased ventricular afterload due to increased ventricle-arterial coupling, resulting in decrease in cardiac output [92]. In addition, Fontan physiology was shown to have deleterious effects on cardiac reserve in response to increased heart rate or β-adrenergic stimulation [92]. The atrium of single ventricle appear to represent early ventricular diastolic dysfunction by atrial dilatation, decreased atrial compliance, decreased early diastolic emptying, and increased reliance on active atrial contraction for ventricular filling [93]. An inverse relationship between ventricular sphericity and global circumferential strain of the single ventricle was observed in Fontan patients, suggesting its limited compensatory mechanisms for increased afterload due to altered geometry and fiber orientation [94].

4-2 Pulmonary Hypertension and RV Dysfunction

Pulmonary hypertension is a hemodynamic and pathophysiologic condition defined as an increase in mean pulmonary artery pressure of ≥25 mmHg at rest as assessed by right-heart catheterization. In patients with pulmonary hypertension, assessment of RV function plays a very important role in prognostication and assessment of response to therapy [95]. Due to ease of access and cost, echocardiography remains the most vital tool for assessment of RV function. It provides a comprehensive assessment of RV structure, morphology, loading conditions, pulmonary vascular hemodynamics, and RV performance [96, 97].

Echocardiographic assessment of pulmonary hypertension consists of 1) hemodynamic assessment of RV afterload, 2) global and regional functional assessment of RV, and 3) volumetric assessment of RV [96, 98].

4-2-1 *Assessment of Increased RV Afterload*

Chronic pulmonary hypertension leads to an increased afterload on the RV. This results in the echocardiographic findings of RV hypertrophy, increased interventricular septal thickness, reduced global RV systolic function, and enlarged right-side chambers. Systolic and diastolic RV pressure can be estimated by pulsed/ continuous wave Doppler assessment of tricuspid regurgitation and pulmonary regurgitation, respectively. Pulmonary hypertension induces a unique RV remodeling pattern different from other chronic RV pressure overload models (valvar pulmonary stenosis and systemic RV) with poorer global function, probably mediated by higher degree of interventricular dyssynchrony [99]. Furthermore, the abnormal pressure gradient between the LV and RV results in a flattened position of the interventricular septum that persists throughout the cardiac cycle [95]. End systolic septal flattening and eccentricity index >1 is suggestive of worsening pulmonary hypertension. The eccentricity index is measured in the parasaternal short axis at the level of the papillary muscles. Significant systolic septal bowing of the interventricular septum onto the LV results in decreased LV stroke volume and cardiac output [100]. Elevated RV afterload is also qualitatively assessed by the morphological changes of RV, shape of interventricular septum, and dilatation of RA and RV.

4-2-2 *Assessment of Myocardial Performance and RV function*

Right ventricle dysfunction is a well-established prognostic marker of pulmonary hypertension [101]. Of the commonly used indices previously described, RV myocardial performance index, RV fractional area change, tricuspid annular plane systolic excursion and S' velocity obtained by TDI remain the primary tools for assessment of RV function in children with PH [30, 33, 102]. The RV fractional area change may be difficult to measure as it measures the area change of the inflow and the trabeculated portions of the RV and does not include the outflow portion, which is in a different echocardiographic plane. Tricuspid annular plane systolic excursion and *S*' represent long-axial contraction from the apex toward the tricuspid annuls and are susceptible to changes due to volume loading. In patients with pulmonary hypertension, they may be affected by the severity of tricuspid regurgitation [103]. On the other hand, RV myocardial performance index is not influenced by the morphological features as it is measured from blood flow waveforms at the inflow and outflow tracts [104] and is a useful predictor of outcome in patients with pulmonary hypertension [105]. Measurement of the *S'*, a maximum velocity of tricuspid valve excursion at the free-wall side using tissue Doppler imaging, is also useful in assessment of RV function in children with pulmonary hypertension. The normal range of S' is 10–19 cm/sec; S' < 11 cm/sec is thought to reflect impaired right cardiac function [102].

The measurement of RV longitudinal strain by 2-dimensional-speckle tracking echocardiography is useful for estimating global and regional systolic RV function in children with PH. The angle-independent nature of this measurement and the ability to assess multiple segments of the RV may make it better than some of the more conventional indices of RV function [106]. For RV strain, a 6-segment RV model is typically described (basal RV free wall, mid RV free wall, apical RV wall, apical septum, mid-septum, and basal septum). The ventricular septum is shared between the two ventricles and reflects both

RV and LV contractility, thus making the septal RV longitudinal strain values difficult to interpret [107]. Jone et al. demonstrated 3-dimensional RV ejection fraction is an outcome predictor whereas RV strain is a more sensitive indicator of function and direct measure of myocardial performance [108]. In adult patients with idiopathic pulmonary hypertension, Filusch et al. found significant correlation between TDI strain and strain rate of RV and different parameters of functional assessment including 6-minute walk distance, N-terminal pro B-type natriuretic peptide (NT-ProBNP), and right heart catheterization values [109]. Speckle tracking echocardiography-derived assessment of RV dyssynchrony, which detects regional differences between apical, mid, and base segments, provided excellent prediction of aerobic exercise capacity in adults with idiopathic pulmonary hypertension [110].

Assessment of RV diastolic function is carried out by pulsed Doppler of the tricuspid inflow, tissue Doppler of the lateral tricuspid annulus, pulsed Doppler of the hepatic vein, and measurements of RA and inferior vena cava sizes and their collapsibility. The E/A ratio, the E/e′ ratio, and size of RA and RV can be used to give an idea of RV diastolic function [100]. Midterm RV and RA reverse remodeling, reduction in size of RA and RV, plays an important role in disease progression and prognosis for pulmonary hypertension patients; more than 15% decrease of RA area and RV end-systolic area with treatment predicted better hemodynamic parameters and survival [111]. The RA has a simpler chamber geometry and structure, and its functional analysis by strain and SR may afford an indirect but easier measure of RV function in pulmonary hypertension. Poorer RA function indicated by strain and strain rate analysis was associated with a worse outcome in patients with pulmonary hypertension [112].

4-2-3 *RV Volume*

Dilation of the RV is an early maladaptive change to increase in pulmonary hypertension [113]. Two-dimensional echocardiographic methods of analyzing RV performance employ geometric models that do not represent the irregular RV shape accurately. Real-time 3-dimensional echocardiography allows reliable measurement of RV end-diastolic volume and ejection fraction, regardless of its shape.

Right ventricle volumes calculated from real time 3-dimensional echocardiography showed significantly better agreement and lower intraobserver and interobserver variability than those calculated from 2-dimensional echocardiography with accuracy comparable to cardiac magnetic resonance imaging [108, 114]. Right ventricle quantification using single-beat 3-dimensional RV ejection fraction was shown to be a superior method in estimating RV function as it correlated better with serum brain natriuretic peptide (BNP) level and hemodynamic parameters obtained by cardiac catheterization when compared with 2-dimensional echocardiographic parameters including fractional area change, tricuspid annular plane systolic excursion, and RV myocardial performance imaging [115].

4-2-4 *RV Interaction with Other Cardiac Chambers in Pulmonary Hypertension*

Dilated and hypertensive RV in advanced pulmonary hypertension is commonly related to underfilling and dysfunction of compressed LV [116]. Dysfunctional RV not only fails to supply adequate LV preload but also impedes LV filling through direct compression [117]. Motoji et al. demonstrated that RV systolic function determined by RV free-wall strain correlated well with LV filling estimated by early diastolic transmitral velocity (E') and that both RV systolic dysfunction and LV under-filling were associated with poor prognosis [118]. The impact of RV pressure overload on LV systolic function in pulmonary hypertension patients was studied with LV strain by speckle tracking echocardiography, which showed impaired LV contractility despite preserved LV ejection fraction, suggesting subclinical LV dysfunction possibly as an effect of ventricular interdependence (see 4-3 Ventricular-Ventricular Interaction). Global LV longitudinal strain was associated independently with RV function assessed by fractional area change and tricuspid annular plane systolic excursion [119].

4-3 Ventricular-Ventricular Interaction

Ventricular-ventricular interaction is the effect of one ventricular function and morphology on the other ventricle. It has been known that acute changes in right ventricular pressure affect left ventricular function [120], in which both direct interactions and interaction in series play a role. The direct interactions are related to shared ventricular septum, the pericardium, and shared myocardial fibers between the two ventricles as well as mechanical asynchrony [121]. The series interaction is related mainly to effect of RV output on the LV preload [122]. One effect of RV pressure and/or volume overload is the ventricular septal shift and D-shaped ventricular septal contour, which can be quantified by echocardiogram with the eccentricity index, a ratio of lateral to antero-posterior LV dimensions. The ratio of RV to LV dimensions in short axis view > 1 at end systole has been associated with adverse clinical outcomes in children with PH [123].

Comparing echocardiographic LV deformation with cardiac MRI and exercise data, Cheung et al showed that LV deformation is impaired in patients with TOF when compared with controls and that circumferential deformation of the LV is inversely correlated with RV end systolic volume and positively correlated with exercise capacity [124]. In severely pressure-loaded RV, there is prolongation of RV systole and shortened diastolic filling, which have direct effects (septal shift and impaired LV filling) [116] and indirect effects (decreased RV output and decreased LV filling and preload) [125]. This even affects LV diastolic function indices like reversed ratio of mitral early diastolic, E, to atrial contraction, A, velocities [116, 117]. In patients with repaired tetralogy of Fallot, LV end diastolic and end systolic dimension Z scores correlated inversely with presence of pulmonary valve regurgitation and reached scores of the normal population after pulmonary valve replacement [126]. There is also decreased LV longitudinal and circumferential strain when compared with the normal population [127]. Adult patients with repaired tetralogy of Fallot not only have reduced RV free-wall longitudinal strain, but also reduced LV free-wall longitudinal strain, radial and circumferential strain, and RV-indexed volume by cardiac magnetic resonance correlated with abnormal basal rotation of the LV [128]. Ventricular dyssynchrony may play a role in ventricular-ventricular interaction as shown in a study of adult patients with repaired tetralogy of Fallot in which increased peak-to-peak systolic time delays as measured by strain imaging correlated with LV ejection fraction, QRS duration, and risk of arrhythmias [129].

5 Conclusion

Echocardiography is the first-line imaging modality of choice used for morphological assessment of cardiac anatomy by real-time imaging in pediatric cardiology. It also provides functional assessment of hemodynamic status, ventricular myocardial performance, and clinical outcome through systolic and diastolic indices and hemodynamic parameters. Emerging new echocardiographic technologies, including 3-dimensional echocardiography, tissue Doppler imaging, speckle tracking echocardiography, and others have now become incorporated into routine examinations focused on assessment of ventricular performance. Advanced imaging modalities such as magnetic resonance imaging and computed tomography are often used in conjunction with echocardiography to enhance accuracy of diagnosis. It is imperative for pediatric cardiologists to become familiar with methodology, clinical applications, and potential limitations of these advanced echocardiographic modalities. To make a final conclusion for ventricular function in variable situations by echocardiography, it is essential to apply these multidisciplinary methods in synergy, including subjective systolic and diastolic assessment.

6. References

[1] Lopez L, Colan SD, Frommelt PC, Ensing GJ, Kendall K, Younoszai AK, et al. Recommendations for quantification methods during the performance of a pediatric echocardiogram: a report from the Pediatric Measurements Writing Group of the American Society of Echocardiography Pediatric and Congenital Heart Disease Council. J Am Soc Echocardiogr. 2010;23:465-95; quiz 576-7.

[2] Frommelt PC, Minich LL, Trachtenberg FL, Altmann K, Camarda J, Cohen MS, et al. Challenges With Left Ventricular Functional Parameters: The Pediatric Heart Network Normal Echocardiogram Database. J Am Soc Echocardiogr. 2019;32:1331-8 e1.

[3] Mertens LF, MK. Systolic ventricular function. In: Lai WM, LL; Cohen MS; Geva T, editor. Echocardiography in pediatric and congenital heart disease: From fetus to adult 2nd ed: Wiely & Sons, Ltd.; 2016. p. 96-131.

[4] Lang RM, Badano LP, Mor-Avi V, Afilalo J, Armstrong A, Ernande L, et al. Recommendations for cardiac chamber quantification by echocardiography in adults: an update from the American Society of Echocardiography and the European Association of Cardiovascular Imaging. J Am Soc Echocardiogr. 2015;28:1-39 e14.

[5] Chengode S. Left ventricular global systolic function assessment by echocardiography. Ann Card Anaesth. 2016;19:S26-S34.

[6] Sisson DD, Daniel GB, Twardock AR. Comparison of left ventricular ejection fractions determined in healthy anesthetized dogs by echocardiography and gated equilibrium radionuclide ventriculography. Am J Vet Res. 1989;50:1840-7.

[7] Tsuda T, Kharouf, R., Prada-Ruiz, A.C.; Baffa, J.M. . Recognition and Management of Preclinical Cardiomyopathies in Children: Special Focus on Duchenne Muscular Dystrophy and Anthracycline Cardiotoxicity. Journal of Pediatric Cardiology and Cardiac Surgery. 2019:63-79.

[8] Echocardiography in Pediatric and Congenital Heart Disease: From Fetus to Adult. Second ed: John Wiley & Sons Ltd; 2016.

[9] Lee SCSN, JC, Roytman, Z; Ko, HH; Lytrivi, ID, Srivastava S. Comparison of two-dimensional echocardiography methods of ventricular volume quantification to cardiovascular magnetic resonance in left ventricular volume overload. Progress in Pediatric Cardiology. 2017;46:57-64.

[10] Lu JC, Ensing GJ, Yu S, Thorsson T, Donohue JE, Dorfman AL. 5/6 Area length method for left-ventricular ejection-fraction measurement in adults with repaired tetralogy of Fallot: comparison with cardiovascular magnetic resonance. Pediatr Cardiol. 2013;34:231-9.

[11] Friedberg MK, Silverman NH. Cardiac ventricular diastolic and systolic duration in children with heart failure secondary to idiopathic dilated cardiomyopathy. Am J Cardiol. 2006;97:101-5.

[12] Tissot C, Singh Y, Sekarski N. Echocardiographic Evaluation of Ventricular Function-For the Neonatologist and Pediatric Intensivist. Front Pediatr. 2018;6:79.

[13] Tei C, Ling LH, Hodge DO, Bailey KR, Oh JK, Rodeheffer RJ, et al. New index of combined systolic and diastolic myocardial performance: a simple and reproducible measure of cardiac function--a study in normals and dilated cardiomyopathy. J Cardiol. 1995;26:357-66.

[14] Nishimura RA, Housmans PR, Hatle LK, Tajik AJ. Assessment of diastolic function of the heart: background and current applications of Doppler echocardiography. Part I. Physiologic and pathophysiologic features. Mayo Clin Proc. 1989;64:71-81.

[15] Appleton CP, Jensen JL, Hatle LK, Oh JK. Doppler evaluation of left and right ventricular diastolic function: a technical guide for obtaining optimal flow velocity recordings. J Am Soc Echocardiogr. 1997;10:271-92.

[16] Courtois M, Vered Z, Barzilai B, Ricciotti NA, Perez JE, Ludbrook PA. The transmitral pressure-flow velocity relation. Effect of abrupt preload reduction. Circulation. 1988;78:1459-68.

[17] Keren G, Sherez J, Megidish R, Levitt B, Laniado S. Pulmonary venous flow pattern--its relationship to cardiac dynamics. A pulsed Doppler echocardiographic study. Circulation. 1985;71:1105-12.

[18] Nagueh SF, Smiseth OA, Appleton CP, Byrd BF, 3rd, Dokainish H, Edvardsen T, et al. Recommendations for the Evaluation of Left Ventricular Diastolic Function by Echocardiography: An

Update from the American Society of Echocardiography and the European Association of Cardiovascular Imaging. J Am Soc Echocardiogr. 2016;29:277-314.

[19] Rossvoll O, Hatle LK. Pulmonary venous flow velocities recorded by transthoracic Doppler ultrasound: relation to left ventricular diastolic pressures. J Am Coll Cardiol. 1993;21:1687-96.

[20] Brun P, Tribouilloy C, Duval AM, Iserin L, Meguira A, Pelle G, et al. Left ventricular flow propagation during early filling is related to wall relaxation: a color M-mode Doppler analysis. J Am Coll Cardiol. 1992;20:420-32.

[21] Garcia MJ, Ares MA, Asher C, Rodriguez L, Vandervoort P, Thomas JD. An index of early left ventricular filling that combined with pulsed Doppler peak E velocity may estimate capillary wedge pressure. J Am Coll Cardiol. 1997;29:448-54.

[22] Dragulescu A, Mertens L, Friedberg MK. Interpretation of left ventricular diastolic dysfunction in children with cardiomyopathy by echocardiography: problems and limitations. Circ Cardiovasc Imaging. 2013;6:254-61.

[23] Abdurrahman L, Hoit BD, Banerjee A, Khoury PR, Meyer RA. Pulmonary venous flow Doppler velocities in children. J Am Soc Echocardiogr. 1998;11:132-7.

[24] Eidem BW, McMahon CJ, Cohen RR, Wu J, Finkelshteyn I, Kovalchin JP, et al. Impact of cardiac growth on Doppler tissue imaging velocities: a study in healthy children. J Am Soc Echocardiogr. 2004;17:212-21.

[25] O'Leary PW, Durongpisitkul K, Cordes TM, Bailey KR, Hagler DJ, Tajik J, et al. Diastolic ventricular function in children: a Doppler echocardiographic study establishing normal values and predictors of increased ventricular end-diastolic pressure. Mayo Clin Proc. 1998;73:616-28.

[26] Sasaki N, Garcia M, Ko HH, Sharma S, Parness IA, Srivastava S. Applicability of published guidelines for assessment of left ventricular diastolic function in adults to children with restrictive cardiomyopathy: an observational study. Pediatr Cardiol. 2015;36:386-92.

[27] Haddad F, Hunt SA, Rosenthal DN, Murphy DJ. Right ventricular function in cardiovascular disease, part I: Anatomy, physiology, aging, and functional assessment of the right ventricle. Circulation. 2008;117:1436-48.

[28] Kamra K, Punn R. Role of echocardiography in the assessment of right ventricular function in the pediatric population. Paediatr Anaesth. 2019;29:530-8.

[29] Breatnach CR, Levy PT, James AT, Franklin O, El-Khuffash A. Novel Echocardiography Methods in the Functional Assessment of the Newborn Heart. Neonatology. 2016;110:248-60.

[30] Amano H, Abe S, Hirose S, Waku R, Masuyama T, Sakuma M, et al. Comparison of echocardiographic parameters to assess right ventricular function in pulmonary hypertension. Heart Vessels. 2017;32:1214-9.

[31] Ishii M, Eto G, Tei C, Tsutsumi T, Hashino K, Sugahara Y, et al. Quantitation of the global right ventricular function in children with normal heart and congenital heart disease: a right ventricular myocardial performance index. Pediatr Cardiol. 2000;21:416-21.

[32] Eidem BW, O'Leary PW, Tei C, Seward JB. Usefulness of the myocardial performance index for assessing right ventricular function in congenital heart disease. Am J Cardiol. 2000;86:654-8.

[33] Kaul S, Tei C, Hopkins JM, Shah PM. Assessment of right ventricular function using two-dimensional echocardiography. Am Heart J. 1984;107:526-31.

[34] Nunez-Gil IJ, Rubio MD, Carton AJ, Lopez-Romero P, Deiros L, Garcia-Guereta L, et al. Determination of normalized values of the tricuspid annular plane systolic excursion (TAPSE) in 405 Spanish children and adolescents. Rev Esp Cardiol. 2011;64:674-80.

[35] Jenkins C, Bricknell K, Hanekom L, Marwick TH. Reproducibility and accuracy of echocardiographic measurements of left ventricular parameters using real-time three-dimensional echocardiography. 2004;44:878-86.

[36] Dorosz JL, Lezotte DC, Weitzenkamp DA, Allen LA, Salcedo EE. Performance of 3-Dimensional Echocardiography in Measuring Left Ventricular Volumes and Ejection Fraction. Journal of the American College of Cardiology. 2012;59:1799-808.

[37] Muraru D, Cecchetto A, Cucchini U, Zhou X, Lang RM, Romeo G, et al. Intervendor Consistency and Accuracy of Left Ventricular Volume Measurements Using Three-Dimensional Echocardiography. Journal of the American Society of Echocardiography. 2018;31:158-68.e1.

[38] Hoffmann R, Barletta G, Von Bardeleben S, Vanoverschelde JL, Kasprzak J, Greis C, et al. Analysis of Left Ventricular Volumes and Function: A Multicenter Comparison of Cardiac Magnetic Resonance Imaging, Cine Ventriculography, and Unenhanced and Contrast-Enhanced Two-Dimensional and Three-Dimensional Echocardiography. Journal of the American Society of Echocardiography. 2014;27:292-301.

[39] Simpson J, Lopez L, Acar P, Friedberg MK, Khoo NS, Ko HH, et al. Three-dimensional Echocardiography in Congenital Heart Disease: An Expert Consensus Document from the European Association of Cardiovascular Imaging and the American Society of Echocardiography. Journal of the American Society of Echocardiography. 2017;30:1-27.

[40] Bellsham-Revell HR, Simpson JM, Miller OI, Bell AJ. Subjective evaluation of right ventricular systolic function in hypoplastic left heart syndrome: how accurate is it? J Am Soc Echocardiogr. 2013;26:52-6.

[41] Simpson JM, Van Den Bosch A. EDUCATIONAL SERIES IN CONGENITAL HEART DISEASE: Three-dimensional echocardiography in congenital heart disease. Echo Research and Practice. 2019;6:R75-R86.

[42] Kapetanakis S, Kearney MT, Siva A, Gall N, Cooklin M, Monaghan MJ. Real-Time Three-Dimensional Echocardiography. Circulation. 2005;112:992-1000.

[43] Nagueh SF, Middleton KJ, Kopelen HA, Zoghbi WA, Quinones MA. Doppler tissue imaging: a noninvasive technique for evaluation of left ventricular relaxation and estimation of filling pressures. J Am Coll Cardiol. 1997;30:1527-33.

[44] Mirsky I, Parmley WW. Assessment of passive elastic stiffness for isolated heart muscle and the intact heart. Circ Res. 1973;33:233-43.

[45] Axel L, Dougherty L. MR imaging of motion with spatial modulation of magnetization. Radiology. 1989;171:841-5.

[46] Zerhouni EA, Parish DM, Rogers WJ, Yang A, Shapiro EP. Human heart: tagging with MR imaging--a method for noninvasive assessment of myocardial motion. Radiology. 1988;169:59-63.

[47] D'Hooge J, Heimdal A, Jamal F, Kukulski T, Bijnens B, Rademakers F, et al. Regional strain and strain rate measurements by cardiac ultrasound: principles, implementation and limitations. Eur J Echocardiogr. 2000;1:154-70.

[48] Leung DY, Ng AC. Emerging clinical role of strain imaging in echocardiography. Heart Lung Circ. 2010;19:161-74.

[49] Yip G, Abraham T, Belohlavek M, Khandheria BK. Clinical applications of strain rate imaging. J Am Soc Echocardiogr. 2003;16:1334-42.

[50] Heimdal A, Stoylen A, Torp H, Skjaerpe T. Real-time strain rate imaging of the left ventricle by ultrasound. J Am Soc Echocardiogr. 1998;11:1013-9.

[51] Dalen H, Thorstensen A, Aase SA, Ingul CB, Torp H, Vatten LJ, et al. Segmental and global longitudinal strain and strain rate based on echocardiography of 1266 healthy individuals: the HUNT study in Norway. Eur J Echocardiogr. 2010;11:176-83.

[52] Weidemann F, Eyskens B, Jamal F, Mertens L, Kowalski M, D'Hooge J, et al. Quantification of regional left and right ventricular radial and longitudinal function in healthy children using ultrasound-based strain rate and strain imaging. J Am Soc Echocardiogr. 2002;15:20-8.

[53] Yingchoncharoen T, Agarwal S, Popovic ZB, Marwick TH. Normal ranges of left ventricular strain: a meta-analysis. J Am Soc Echocardiogr. 2013;26:185-91.

[54] Levy PT, Machefsky A, Sanchez AA, Patel MD, Rogal S, Fowler S, et al. Reference Ranges of Left Ventricular Strain Measures by Two-Dimensional Speckle-Tracking Echocardiography in Children: A Systematic Review and Meta-Analysis. J Am Soc Echocardiogr. 2016;29:209-25 e6.

[55] Levy PT, Sanchez Mejia AA, Machefsky A, Fowler S, Holland MR, Singh GK. Normal ranges of right ventricular systolic and diastolic strain measures in children: a systematic review and meta-analysis. J Am Soc Echocardiogr. 2014;27:549-60, e3.

[56] Sehgal S, Blake JM, Sommerfield J, Aggarwal S. Strain and strain rate imaging using speckle tracking in acute allograft rejection in children with heart transplantation. Pediatr Transplant. 2015;19:188-95.

[57] Mavinkurve-Groothuis AM, Marcus KA, Pourier M, Loonen J, Feuth T, Hoogerbrugge PM, et al. Myocardial 2D strain echocardiography and cardiac biomarkers in children during and shortly after anthracycline therapy for acute lymphoblastic leukaemia (ALL): a prospective study. Eur Heart J Cardiovasc Imaging. 2013;14:562-9.

[58] Taqatqa A, Bokowski J, Al-Kubaisi M, Khalil A, Miranda C, Alaksham H, et al. The Use of Speckle Tracking Echocardiography for Early Detection of Myocardial Dysfunction in Patients with Duchenne Muscular Dystrophy. Pediatr Cardiol. 2016;37:1422-8.

[59] Perdreau E, Seguela PE, Jalal Z, Perdreau A, Mouton JB, Nelson-Veniard M, et al. Postoperative assessment of left ventricular function by two-dimensional strain (speckle tracking) after paediatric cardiac surgery. Arch Cardiovasc Dis. 2016;109:599-606.

[60] Notomi Y, Lysyansky P, Setser RM, Shiota T, Popovic ZB, Martin-Miklovic MG, et al. Measurement of ventricular torsion by two-dimensional ultrasound speckle tracking imaging. J Am Coll Cardiol. 2005;45:2034-41.

[61] Notomi Y, Srinath G, Shiota T, Martin-Miklovic MG, Beachler L, Howell K, et al. Maturational and adaptive modulation of left ventricular torsional biomechanics: Doppler tissue imaging observation from infancy to adulthood. Circulation. 2006;113:2534-41.

[62] Jin SM, Noh CI, Bae EJ, Choi JY, Yun YS. Decreased left ventricular torsion and untwisting in children with dilated cardiomyopathy. J Korean Med Sci. 2007;22:633-40.

[63] Jashari H, Rydberg A, Ibrahimi P, Bajraktari G, Henein MY. Left ventricular response to pressure afterload in children: aortic stenosis and coarctation: a systematic review of the current evidence. Int J Cardiol. 2015;178:203-9.

[64] Cheung YF, Li SN, Chan GC, Wong SJ, Ha SY. Left ventricular twisting and untwisting motion in childhood cancer survivors. Echocardiography. 2011;28:738-45.

[65] Delmo Walter EM, Hubler M, Alexi-Meskishvili V, Miera O, Weng Y, Loforte A, et al. Staged surgical palliation in hypoplastic left heart syndrome and its variants. J Card Surg. 2009;24:383-91.

[66] Jolley M, Colan SD, Rhodes J, DiNardo J. Fontan physiology revisited. Anesth Analg. 2015;121:172-82.

[67] Durongpisitkul K, Driscoll DJ, Mahoney DW, Wollan PC, Mottram CD, Puga FJ, et al. Cardiorespiratory response to exercise after modified Fontan operation: determinants of performance. J Am Coll Cardiol. 1997;29:785-90.

[68] Czosek RJ, Anderson JB, Heaton PC, Cassedy A, Schnell B, Cnota JF. Staged palliation of hypoplastic left heart syndrome: trends in mortality, cost, and length of stay using a national database from 2000 through 2009. Am J Cardiol. 2013;111:1792-9.

[69] Lopez L, Cohen MS, Anderson RH, Redington AN, Nykanen DG, Penny DJ, et al. Unnatural history of the right ventricle in patients with congenitally malformed hearts. Cardiol Young. 2010;20 Suppl 3:107-12.

[70] Anderson PA, Sleeper LA, Mahony L, Colan SD, Atz AM, Breitbart RE, et al. Contemporary outcomes after the Fontan procedure: a Pediatric Heart Network multicenter study. J Am Coll Cardiol. 2008;52:85-98.

[71] Friedberg MK, Silverman NH, Dubin AM, Rosenthal DN. Right ventricular mechanical dyssynchrony in children with hypoplastic left heart syndrome. J Am Soc Echocardiogr. 2007;20:1073-9.

[72] Rosner A, Khalapyan T, Dalen H, McElhinney DB, Friedberg MK, Lui GK. Classic-Pattern Dyssynchrony in Adolescents and Adults With a Fontan Circulation. J Am Soc Echocardiogr. 2018;31:211-9.

[73] Schlangen J, Fischer G, Petko C, Hansen JH, Voges I, Rickers C, et al. Arterial elastance and its impact on intrinsic right ventricular function in palliated hypoplastic left heart syndrome. Int J Cardiol. 2013;168:5385-9.

[74] Kutty S, Rathod RH, Danford DA, Celermajer DS. Role of imaging in the evaluation of single ventricle with the Fontan palliation. Heart. 2016;102:174-83.

[75] Hershenson JA, Zaidi AN, Texter KM, Moiduddin N, Stefaniak CA, Hayes J, et al. Differences in tissue Doppler imaging between single ventricles after the fontan operation and normal controls. Am J Cardiol. 2010;106:99-103.

[76] Lopez C, Mertens L, Dragulescu A, Landeck B, Younoszai A, Friedberg MK, et al. Strain and Rotational Mechanics in Children With Single Left Ventricles After Fontan. J Am Soc Echocardiogr. 2018;31:1297-306.

[77] Moiduddin N, Texter KM, Zaidi AN, Hershenson JA, Stefaniak C, Hayes J, et al. Two-dimensional speckle strain and dyssynchrony in single left ventricles vs. normal left ventricles. Congenit Heart Dis. 2010;5:579-86.

[78] Ho PK, Lai CT, Wong SJ, Cheung YF. Three-dimensional mechanical dyssynchrony and myocardial deformation of the left ventricle in patients with tricuspid atresia after Fontan procedure. J Am Soc Echocardiogr. 2012;25:393-400.

[79] Zhang S, Liu X, Bawa-Khalfe T, Lu LS, Lyu YL, Liu LF, et al. Identification of the molecular basis of doxorubicin-induced cardiotoxicity. Nat Med. 2012;18:1639-42.

[80] Moiduddin N, Texter KM, Zaidi AN, Hershenson JA, Stefaniak CA, Hayes J, et al. Two-dimensional speckle strain and dyssynchrony in single right ventricles versus normal right ventricles. J Am Soc Echocardiogr. 2010;23:673-9.

[81] Kaneko S, Khoo NS, Smallhorn JF, Tham EB. Single right ventricles have impaired systolic and diastolic function compared to those of left ventricular morphology. J Am Soc Echocardiogr. 2012;25:1222-30.

[82] West C, Maul T, Feingold B, Morell VO. Right Ventricular Dominance Is Associated With Inferior Outcomes After the Extracardiac Fontan. World J Pediatr Congenit Heart Surg. 2019;10:416-23.

[83] Zaidi SJ, Penk J, Cui VW, Kanjanauthai S, Roberson DA. Right Ventricular Systolic Function Parameters in Hypoplastic Left Heart Syndrome. Pediatr Cardiol. 2018;39:1423-32.

[84] Schlangen J, Petko C, Hansen JH, Michel M, Hart C, Uebing A, et al. Two-dimensional global longitudinal strain rate is a preload independent index of systemic right ventricular contractility in hypoplastic left heart syndrome patients after Fontan operation. Circ Cardiovasc Imaging. 2014;7:880-6.

[85] Grattan M, Mertens L, Grosse-Wortmann L, Friedberg MK, Cifra B, Dragulescu A. Ventricular Torsion in Young Patients With Single-Ventricle Anatomy. J Am Soc Echocardiogr. 2018;31:1288-96.

[86] Sato T, Calderon RJ, Klas B, Pedrizzetti G, Banerjee A. Simultaneous Volumetric and Functional Assessment of the Right Ventricle in Hypoplastic Left Heart Syndrome After Fontan Palliation, Utilizing 3-Dimensional Speckle-Tracking Echocardiography. Circ J. 2020;84:235-44.

[87] Olivier M, O'Leary P W, Pankratz VS, Lohse CM, Walsh BE, Tajik AJ, et al. Serial Doppler assessment of diastolic function before and after the Fontan operation. J Am Soc Echocardiogr. 2003;16:1136-43.

[88] Menon SC, Gray R, Tani LY. Evaluation of ventricular filling pressures and ventricular function by Doppler echocardiography in patients with functional single ventricle: correlation with simultaneous cardiac catheterization. J Am Soc Echocardiogr. 2011;24:1220-5.

[89] Goudar SP, Zak V, Atz AM, Altmann K, Colan SD, Falkensammer CB, et al. Comparison of echocardiographic measurements to invasive measurements of diastolic function in infants with single ventricle physiology: a report from the Pediatric Heart Network Infant Single Ventricle Trial. Cardiol Young. 2019;29:1248-56.

[90] Margossian R, Sleeper LA, Pearson GD, Barker PC, Mertens L, Quartermain MD, et al. Assessment of Diastolic Function in Single-Ventricle Patients After the Fontan Procedure. J Am Soc Echocardiogr. 2016;29:1066-73.

[91] Logoteta J, Ruppel C, Hansen JH, Fischer G, Becker K, Kramer HH, et al. Ventricular function and ventriculo-arterial coupling after palliation of hypoplastic left heart syndrome: A comparative study with Fontan patients with LV morphology. Int J Cardiol. 2017;227:691-7.

[92] Senzaki H, Masutani S, Ishido H, Taketazu M, Kobayashi T, Sasaki N, et al. Cardiac rest and reserve function in patients with Fontan circulation. J Am Coll Cardiol. 2006;47:2528-35.

[93] Khoo NS, Smallhorn JF, Kaneko S, Kutty S, Altamirano L, Tham EB. The assessment of atrial function in single ventricle hearts from birth to Fontan: a speckle-tracking study by using strain and strain rate. J Am Soc Echocardiogr. 2013;26:756-64.
[94] Rosner A, Khalapyan T, Pedrosa J, Dalen H, McElhinney DB, Friedberg MK, et al. Ventricular mechanics in adolescent and adult patients with a Fontan circulation: Relation to geometry and wall stress. Echocardiography. 2018;35:2035-46.
[95] Wright LM, Dwyer N, Celermajer D, Kritharides L, Marwick TH. Follow-Up of Pulmonary Hypertension With Echocardiography. JACC Cardiovasc Imaging. 2016;9:733-46.
[96] Koestenberger M, Friedberg MK, Nestaas E, Michel-Behnke I, Hansmann G. Transthoracic echocardiography in the evaluation of pediatric pulmonary hypertension and ventricular dysfunction. Pulm Circ. 2016;6:15-29.
[97] Bushby KM, Gardner-Medwin D, Nicholson LV, Johnson MA, Haggerty ID, Cleghorn NJ, et al. The clinical, genetic and dystrophin characteristics of Becker muscular dystrophy. II. Correlation of phenotype with genetic and protein abnormalities. J Neurol. 1993;240:105-12.
[98] Bhattacharya S, Sen S, Levy PT, Rios DR. Comprehensive Evaluation of Right Heart Performance and Pulmonary Hemodynamics in Neonatal Pulmonary Hypertension : Evaluation of cardiopulmonary performance in neonatal pulmonary hypertension. Curr Treat Options Cardiovasc Med. 2019;21:10.
[99] Driessen MMP, Leiner T, Sieswerda GT, van Dijk APJ, Post MC, Friedberg MK, et al. RV adaptation to increased afterload in congenital heart disease and pulmonary hypertension. PLoS One. 2018;13:e0205196.
[100] Rudski LG, Lai WW, Afilalo J, Hua L, Handschumacher MD, Chandrasekaran K, et al. Guidelines for the echocardiographic assessment of the right heart in adults: a report from the American Society of Echocardiography endorsed by the European Association of Echocardiography, a registered branch of the European Society of Cardiology, and the Canadian Society of Echocardiography. J Am Soc Echocardiogr. 2010;23:685-713; quiz 86-8.

[101] Ghio S, Klersy C, Magrini G, D'Armini AM, Scelsi L, Raineri C, et al. Prognostic relevance of the echocardiographic assessment of right ventricular function in patients with idiopathic pulmonary arterial hypertension. Int J Cardiol. 2010;140:272-8.

[102] Pavlicek M, Wahl A, Rutz T, de Marchi SF, Hille R, Wustmann K, et al. Right ventricular systolic function assessment: rank of echocardiographic methods vs. cardiac magnetic resonance imaging. Eur J Echocardiogr. 2011;12:871-80.

[103] Hsiao SH, Lin SK, Wang WC, Yang SH, Gin PL, Liu CP. Severe tricuspid regurgitation shows significant impact in the relationship among peak systolic tricuspid annular velocity, tricuspid annular plane systolic excursion, and right ventricular ejection fraction. J Am Soc Echocardiogr. 2006;19:902-10.

[104] Tei C, Dujardin KS, Hodge DO, Bailey KR, McGoon MD, Tajik AJ, et al. Doppler echocardiographic index for assessment of global right ventricular function. J Am Soc Echocardiogr. 1996;9:838-47.

[105] Yeo TC, Dujardin KS, Tei C, Mahoney DW, McGoon MD, Seward JB. Value of a Doppler-derived index combining systolic and diastolic time intervals in predicting outcome in primary pulmonary hypertension. Am J Cardiol. 1998;81:1157-61.

[106] Li Y, Wang Y, Meng X, Zhu W, Lu X. Assessment of right ventricular longitudinal strain by 2D speckle tracking imaging compared with RV function and hemodynamics in pulmonary hypertension. Int J Cardiovasc Imaging. 2017;33:1737-48.

[107] Buckberg G, Hoffman JI. Right ventricular architecture responsible for mechanical performance: unifying role of ventricular septum. J Thorac Cardiovasc Surg. 2014;148:3166-71 e1-4.

[108] Jone PN, Schafer M, Pan Z, Bremen C, Ivy DD. 3D echocardiographic evaluation of right ventricular function and strain: a prognostic study in paediatric pulmonary hypertension. Eur Heart J Cardiovasc Imaging. 2018;19:1026-33.

[109] Filusch A, Mereles D, Gruenig E, Buss S, Katus HA, Meyer FJ. Strain and strain rate echocardiography for evaluation of right ventricular dysfunction in patients with idiopathic pulmonary arterial hypertension. Clin Res Cardiol. 2010;99:491-8.

[110] Badagliacca R, Papa S, Valli G, Pezzuto B, Poscia R, Reali M, et al. Right ventricular dyssynchrony and exercise capacity in idiopathic pulmonary arterial hypertension. Eur Respir J. 2017;49.

[111] Sano H, Tanaka H, Motoji Y, Fukuda Y, Sawa T, Mochizuki Y, et al. Right ventricular function and right-heart echocardiographic response to therapy predict long-term outcome in patients with pulmonary hypertension. Can J Cardiol. 2015;31:529-36.

[112] D'Alto M, D'Andrea A, Di Salvo G, Scognamiglio G, Argiento P, Romeo E, et al. Right atrial function and prognosis in idiopathic pulmonary arterial hypertension. Int J Cardiol. 2017;248:320-5.

[113] Milan A, Magnino C, Veglio F. Echocardiographic indexes for the non-invasive evaluation of pulmonary hemodynamics. J Am Soc Echocardiogr. 2010;23:225-39; quiz 332-4.

[114] Vitarelli A, Mangieri E, Terzano C, Gaudio C, Salsano F, Rosato E, et al. Three-dimensional echocardiography and 2D-3D speckle-tracking imaging in chronic pulmonary hypertension: diagnostic accuracy in detecting hemodynamic signs of right ventricular (RV) failure. J Am Heart Assoc. 2015;4:e001584.

[115] Jone PN, Patel SS, Cassidy C, Ivy DD. Three-dimensional Echocardiography of Right Ventricular Function Correlates with Severity of Pediatric Pulmonary Hypertension. Congenit Heart Dis. 2016;11:562-9.

[116] Gan C, Lankhaar JW, Marcus JT, Westerhof N, Marques KM, Bronzwaer JG, et al. Impaired left ventricular filling due to right-to-left ventricular interaction in patients with pulmonary arterial hypertension. Am J Physiol Heart Circ Physiol. 2006;290:H1528-33.

[117] Friedberg MK. Imaging Right-Left Ventricular Interactions. JACC Cardiovasc Imaging. 2018;11:755-71.

[118] Motoji Y, Tanaka H, Fukuda Y, Sano H, Ryo K, Imanishi J, et al. Interdependence of right ventricular systolic function and left ventricular filling and its association with outcome for patients with pulmonary hypertension. Int J Cardiovasc Imaging. 2015;31:691-8.

[119] de Amorim Correa R, de Oliveira FB, Barbosa MM, Barbosa JA, Carvalho TS, Barreto MC, et al. Left Ventricular Function in Patients with Pulmonary Arterial Hypertension: The Role of Two-Dimensional Speckle Tracking Strain. Echocardiography. 2016;33:1326-34.

[120] Milstein JM, Bennett SH. Increased right ventricular afterload alters left ventricular function in newborn lambs. Am Heart J. 1987;114:369-77.

[121] Osculati G, Malfatto G, Chianca R, Perego GB. Left-to-right systolic ventricular interaction in patients undergoing biventricular stimulation for dilated cardiomyopathy. J Appl Physiol (1985). 2010;109:418-23.

[122] Friedberg MK, Redington AN. Right versus left ventricular failure: differences, similarities, and interactions. Circulation. 2014;129:1033-44.

[123] Jone PN, Hinzman J, Wagner BD, Ivy DD, Younoszai A. Right ventricular to left ventricular diameter ratio at end-systole in evaluating outcomes in children with pulmonary hypertension. J Am Soc Echocardiogr. 2014;27:172-8.

[124] Cheung EW, Liang XC, Lam WW, Cheung YF. Impact of right ventricular dilation on left ventricular myocardial deformation in patients after surgical repair of tetralogy of fallot. Am J Cardiol. 2009;104:1264-70.

[125] Marcus JT, Gan CT, Zwanenburg JJ, Boonstra A, Allaart CP, Gotte MJ, et al. Interventricular mechanical asynchrony in pulmonary arterial hypertension: left-to-right delay in peak shortening is related to right ventricular overload and left ventricular underfilling. J Am Coll Cardiol. 2008;51:750-7.

[126] Zervan K, Male C, Benesch T, Salzer-Muhar U. Ventricular interaction in children after repair of tetralogy of Fallot: a longitudinal echocardiographic study. Eur J Echocardiogr. 2009;10:641-6.

[127] Kempny A, Diller GP, Orwat S, Kaleschke G, Kerckhoff G, Bunck A, et al. Right ventricular-left ventricular interaction in adults with Tetralogy of Fallot: a combined cardiac magnetic resonance and echocardiographic speckle tracking study. Int J Cardiol. 2012;154:259-64.

[128] Dragulescu A, Friedberg MK, Grosse-Wortmann L, Redington A, Mertens L. Effect of chronic right ventricular volume overload on ventricular interaction in patients after tetralogy of Fallot repair. J Am Soc Echocardiogr. 2014;27:896-902.

[129] Tzemos N, Harris L, Carasso S, Subira LD, Greutmann M, Provost Y, et al. Adverse left ventricular mechanics in adults with repaired tetralogy of Fallot. Am J Cardiol. 2009;103:420-5.

8. Conflict of Interest

This research did not receive any specific grant from funding agencies in the public, commercial or not-for-profit sectors.

Table 1 **Echocardiographic Assessment of Systolic Function**

	SF	2D EF	3D EF	MPI	S'	Annular Plane Excursion	Strain Global longitudinal and Circumferential	S/D ratio
LV (Preserved geometry)	M-mode	Bi-plane Simpson 5/6 Area Length	Y	May be used	Y		Y	
LV (Altered geometry: Septal position not convex)	FAC	5/6 Area Length	Y	May be used	Y		Y	Y
RV	FAC		Y	Y	Y	Y	Y	Y
Single RV					Y		Y	Y
Single LV		5/6 Area Length	Y		Y	Y	Y	Y

SF: shortening fraction, 2D-EF: 2-dimensional ejection fraction, 3D EF: 3-dimensional ejection fraction, MPI: myocardial performance index, S/D ratio: systolic-to-diastolic time duration ratio, LV: left ventricle, Y: yes, FAC: fractional area change, RV: right ventricle.

Table 2 Echocardiographic Assessment of Diastolic Function

	MV E/A	MV E-wave DT	Pulm vein A-rev duration and velocity reversal	LA size	TDI E', L', A'	RA size
LV	Y	Y	Y	Y		
RV	Y	Y	Y		Y	Y
SV		Y	Y			

MV: mitral valve, DT: deceleration time, Pulm vein A-rev duration: pulmonary vein A-wave reversal duration, LA: left atrium, TDI: tissue Doppler imaging, RA: right atrium, LV: left ventricle, Y: yes, RV: right ventricle, SV single ventricle

Author Statement

The contents of this manuscript has never been published before nor is it considered for publication elsewhere. The final version of the revision has been approved by all coauthors.

Takeshi Tsuda, MD

Highlights

- Assessment of ventricular function is an integral part of cardiology practice
- Advanced echocardiographic technology provides significant physiological data
- Speckle tracking echocardiography is a promising new diagnostic modality
- Multimodality approach is warranted for complex cardiac problems in children